Materials Research Bulletin 47 (2012) 2200–2205

Contents lists available at SciVerse ScienceDirect

Materials Research Bulletin

journal homepage: www.elsevier.com/locate/matresbu

# Effect of plasma CVD operating temperature on nanomechanical properties of TiC nanostructured coating investigated by atomic force microscopy

Ali Shanaghi [a,*], Ali Reza Sabour Rouhaghdam [b], Shahrokh Ahangarani [c,*], Paul K. Chu [d]

[a] Materials Engineering Department, Faculty of Engineering, Malayer University, P.O. Box: 95863-65719, Malayer, Iran
[b] Surface Engineering Laboratory, Materials Engineering Department, Faculty of Engineering, Tarbiat Modares University, P.O. Box: 14115-143, Tehran, Iran
[c] Advanced Materials & Renewable Energies Department, Iranian Research Organization for Science and Technology, P.O. Box 15815-3538, Tehran, Iran
[d] Department of Physics & Materials Science, City University of Hong Kong, Tat Chee Avenue, Kowloon, Hong Kong, China

ARTICLE INFO

*Article history:*
Received 18 June 2011
Received in revised form 1 June 2012
Accepted 4 June 2012
Available online 9 June 2012

*Keywords:*
A. Titanium carbides
A. Nanostructured coatings
B. Plasma CVD
C. Nanoindentation
D. Nanomechanical properties

ABSTRACT

The structure, composition, and mechanical properties of nanostructured titanium carbide (TiC) coatings deposited on $H_{11}$ hot-working tool steel by pulsed-DC plasma assisted chemical vapor deposition at three different temperatures are investigated. Nanoindentation and nanoscratch tests are carried out by atomic force microscopy to determine the mechanical properties such as hardness, elastic modulus, surface roughness, and friction coefficient. The nanostructured TiC coatings prepared at 490 °C exhibit lower friction coefficient (0.23) than the ones deposited at 470 and 510 °C. Increasing the deposition temperature reduces the Young's modulus and hardness. The overall superior mechanical properties such as higher hardness and lower friction coefficient render the coatings deposited at 490 °C suitable for wear resistant applications.



## 1. Introduction

Titanium carbide (TiC) coatings are potential materials in many tribological applications because of the high hardness, low friction, and excellent wear resistance [1]. Thermal or plasma chemical vapor deposition is widely used to deposit hard TiC coatings. In CVD, the coatings are usually deposited onto the substrates at a high temperature between 500 and 1050 °C) [2]. Although CVD coatings tend to have good mechanical properties, one of the limitations is that a substrate with a low melting point cannot be used. On the other hand, plasma-assisted chemical vapor deposition (PACVD) can be used to deposit TiC coatings at a much lower temperature. Further studies indicate that the properties of titanium carbide are related to the chemical composition and texture and also affect the adhesion and residual stress in the thin film [2–9].

The field of nanotribology has evolved due to the rapid development of nanotechnology in the past decade. Contacts on most engineering materials surfaces begin with asperities on the nanoscale [10] and so the interactions and tribological response at nanoscale contacts are important to nanotribological studies. There are several methods for this purpose and atomic force microscopy (AFM) can be used to study tribological characteristics on the nanoscale [10–13].

Despite the increasing use of titanium carbide hard coatings, the tribological interface is not fully understood. It is still challenging to deposit TiC coatings on metals because the materials are metastable and the PACVD reactions are quite complicated. Several fabrication parameters such as the temperature, gas ratio, and duty cycle can affect the properties of TiC coatings. Among the various parameters which affect the properties of TiC nanostructured coatings, the operating temperature plays an important role as a kinetic and thermodynamic parameter. It has been shown that the temperature affects the roughness and growth mechanism of the coatings produced by plasma deposition and the uniformity and homogeneity of the coatings can be improved [14–16]. The objective of this study is to evaluate the scratch wear resistance and nanoindentation characteristics of nanostructured TiC coatings fabricated on $H_{11}$ (DIN 1.2343) by PACVD at 470, 490, and 510 °C. The crystalline structure of the coating is determined by X-ray diffraction (XRD) and the surface morphology, roughness, and nanomechanical properties such as Young's modulus and hardness are determined by atomic force microscopy (AFM).

* Corresponding author. Tel.: +98 9188644460; fax: +98 8512221977.
*E-mail addresses:* alishanaghi@gmail.com, a.shanaghi@malayeru.ac.ir (A. Shanaghi), sabour01@modares.ac.ir (A.R.S. Rouhaghdam), sh.ahangarani@gmail.com (S. Ahangarani), paul.chu@cityu.edu.hk (P.K. Chu).

0025-5408/$ – see front matter © 2012 Elsevier Ltd. All rights reserved.
http://dx.doi.org/10.1016/j.materresbull.2012.06.003

**Table 1**
Processing parameters during deposition of $TiC_x$.

| Parameter | Value |
|---|---|
| Pulsed voltage (V) | 590 |
| Pressure (mbar) | 3–10 |
| Duty cycle (%) | 33 |
| Process time (h) | 2 |
| $H_2$ (Nl/min) | 1.6 |
| Ar (Nl/min) | 0.05 |
| $TiCl_4$ (carrier $H_2$) | 0.05 |
| $CH_4$ (Nl/min) | 0.4–3.2 |
| Temperature (°C) | 470, 490, and 510 |

## 2. Materials and methods

The nanostructured TiC coatings were deposited on hot-working die steel grade AISI $H_{11}$ (DIN 1.2343) substrates in a PACVD reactor using a mixture of $TiCl_4$–$CH_4$–$H_2$–Ar precursors. The plasma was sustained by pulsed DC and the pressure in the reactor was 8 mbar. The main deposition conditions are listed in Tables 1 and 2 show the chemical composition of the steel substrate determined by spark emission spectroscopy.

The substrate temperature was controlled by ion bombardment and an auxiliary heating system. Three different temperatures of 470, 490, and 510 °C were selected to investigate the influence of the deposition temperature on the tribological behavior of the nanostructured TiC coatings.

The crystalline structure of the coatings was evaluated by X-ray diffraction (XRD) on a Philips PW-1730 diffractometer in the continuous scanning mode and using Cu $K_\alpha$ radiation ($\lambda$ = 0.154056 nm). The full width at half maximum (FWHM) of the Bragg peaks is used to estimate the grain size according to Scherrer formula [8]:

$$D = \frac{0.9\lambda}{\beta \cos\theta}, \quad (1)$$

where $D$ is the grain size, $\beta$ is the FWHM of the Bragg peak, and $\theta$ is the angle of Bragg peak reflection. The film composition was determined by X-ray photoelectron spectroscopy (XPS, PHI 5802) using monochromatic Al $K_\alpha$ radiation. An argon ion beam was used to sputter about 40 nm of the surface to remove contaminants before the C1s and Ti2p spectra were acquired.

The surface morphology and roughness of the nanostructured TiC coatings were measured by atomic force microscopy (AFM, NanoScope III from Digital Instruments). The nanomechanical properties such as Young's modulus ($E$) and hardness ($H$) were determined by nanoindentation (A Hysitron Inc. TriboScope). Indents were made using a spherical (radius $R$ = 1.0 μm) diamond indenter supplied by Dr. U.D. Hangen, SURFACE, Hückelhoven on the NanoScope III AFM. The indentation time was 10 s and the sensor of the transducer recorded the values at normal force and depth. The contact hardness (Hc) is defined as the hardness at peak load [17,18]:

$$H_c = \frac{P_{max}}{A_c} = \frac{P_{max}}{\alpha_1 (h_c)^2}, \quad (2)$$

where $\alpha_1$ is a non-dimensional geometrical constant $\alpha_1 = \pi \tan^2\omega c$ in which $\omega$ is the inner angle of the effective cone approximating the pyramidal indenter tip geometry. The value of $\alpha_1$ = 24.5 is associated with an ideal Vickers or Berkovich pyramidal indenter with an angle $\omega$ of 70.3°. Five indents were made on every sample to improve the statistics.

**Table 2**
Chemical analysis of AISI H11 by spark emission spectroscopy.

| Composition | C | Si | V | Cr | Mo | Mn | P |
|---|---|---|---|---|---|---|---|
| Weight percent | 0.36 | 0.56 | 0.4 | 4.6 | 0.52 | 0.37 | 0.01 |

The Young's moduli were calculated from the load-displacement curves as follows:

$$\frac{1}{E_r} = \frac{2\beta}{S}\sqrt{\frac{A_c}{\pi}} = \frac{1-\nu_m^2}{E_m} + \frac{1-\nu_i^2}{E_i}. \quad (3)$$

where $A_c$, $E_r$, $S$ and $\beta$ are the actual contact area, reduced elastic modulus for each indenter/specimen combination, measured stiffness, and shape constant of 1 for the Berkovich tip, respectively. The subscript $m$ and $i$ represent the film and indenter tip, respectively, $E$ is the Young's modulus and $\nu$ is Poisson's ratio. The indenter properties used in this study's calculations were $E_i$ = 1140 GPa and $\nu_i$ = 0.07 assuming a Poisson's ratio of $TiC_x$ to be $\nu_m$ = 0.17 [19].

A Hysitron Inc. TriboScope® Nanomechanical Test Instrument with a 2D transducer with the complete software and the diamond indenter was calibrated according to the TriboScope Users Manual [20]. Typical indents with a 142.3° Berkovich and a cono-spherical radius ($R$ = 1.0 μm) indenter were supplied by SURFACE, Hückelhoven. The scratching time was 60 s and the scratching distance was 4 μm. The sensors of the 2D transducer recorded the values of the normal force and lateral force throughout the experiment. The lateral force was averaged using the flat central regions of the scratches (about 67%) neglecting steps, peaks, or depressions that might have arisen due to single cracks that were minimized by the slower scratching if necessary. However, there was no rate dependence in this range. The normal force and lateral (friction) force during the scratch tests were recorded with time.

The adhesion strength was analyzed using a micro-scratch tester with a diamond tip (radius 10 μm) at a sliding speed was

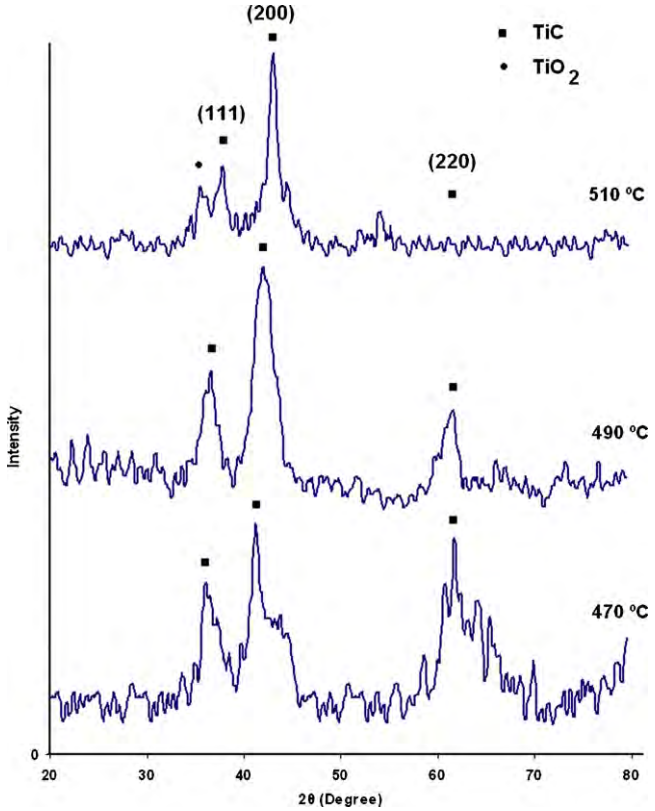


**Fig. 1.** XRD patterns of the TiC coatings deposited by PACVD at 3 different temperatures.

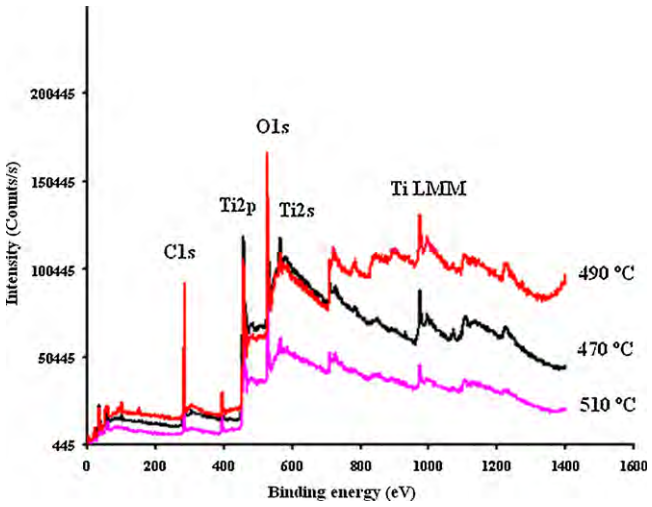


**Fig. 2.** XPS spectra acquired from the surface of the TiC coatings.

15 μm/s. The critical load ($L_c$) was defined as the lowest load at which the $TiC_x$ coatings started to delaminate from the substrate.

## 3. Results and discussion

Fig. 1 shows the XRD diffraction patterns of the coatings deposited at 470, 490 and 510 °C. The reference peaks of TiC are obtained from ICCC-JCPDS (titanium carbide No. 31-1400). The (2 0 0) plane which has the lowest surface energy is the preferred structure [21–23], suggesting that the TiC coating is deposited under stable thermo-dynamical conditions, although the (1 1 1) structure (or texture) is the common structure of TiC. The apparent grain sizes calculated using the Scherrer equation are 13, 7, and 8 nm for the samples prepared at 470, 490, and 510 °C, respectively.

Fig. 2 displays the XPS spectra of the TiC coatings deposited at the three temperatures. The C1 s spectra show a peak at 281.6 eV and $TiO_2$ is indicated by the Ti 2p3/2 peaks at 458.4 eV [24]. The Ti2p and C1s peaks confirm that the coatings are composed of TiC (Table 1). Moreover, no significant variation in the surface chemical composition (C/Ti ratio) is observed for the three temperatures.

Table 3 shows the critical load, $L_c$ (average of 5 measurements) measured on a micro-scratch tester and it is related to the adhesion strength of the nanostructured TiC coatings on the steel substrate. The TiC coating deposited at 510 °C has relatively low adhesion strength compared to the other samples fabricated at 470 and 490 °C. The adhesion strength is improved from 28 mN to 34 mN, but a larger duty cycle reduces the adhesion strength from 34 mN to 21 mN. The adhesion strength decreases with increasing temperature. It can be caused by the internal stress with a high atomic density, structural difference between the films and substrates, inherent brittle properties, or chemical composition [1,25].

The surface morphology and roughness of the three TiC coatings are shown in Fig. 3a–c and the surface roughness results are summarized in Table 3. $R_a$ is defined as the mean value of the surface height relative to the center plane and $R_{rms}$ is the root-mean-square roughness profile of the surface height within the scanned area [26].

Fig. 3 shows that asperities are distributed over a broader range of heights on the samples deposited at 490 °C compared to the ones prepared at 470 °C and 510 °C. This is confirmed by the roughness values. The $R_{rms}$ values of the coatings deposited at 470, 490 and 510 °C are 13.069, 29.781, and 11.668 nm, respectively.

The AFM images and $R_{rms}$ values show that a higher deposition temperature reduces the surface roughness and it is noticeable that the growth mechanism at 490 °C is different from that at 470 and 510 °C. In fact, the dominant mechanism at 490 °C is a layer type, and at 470 and 510 °C, it is an island type (confirmed by the smallest grain size at 490 °C compared those at 470 and 510 °C). In other words, the surface roughness of the coatings produced at 470 and 510 °C is due to the well-known island growth structure of TiC. The results show that $R_a$ and $R_{rms}$ are affected by the structure.

The thickness of the coatings is more than twenty times the total depth of indentation and hence, the hardness and elastic modulus are calculated from the coatings only (no substrate effect). Fig. 4 shows the load–unloading curves obtained from a Berkovich diamond indenter at a load of 2000 μN. The penetration depth in the coating deposited at 490 °C is the smallest and so its hardness is the largest. An unexpected phenomenon at 490 °C at 900 mN may be related to the layer type structure and surface roughness compared to that at 470 and 510 °C, especially on the surface of coatings. The effect disappears at depths over 30 nm.

The hardness versus deposition temperature relationship is shown in Fig. 5. The hardness of the coating reaches a maximum of 16.62 GPa at 490 °C and then decreases at 510 °C, implying that the hardness is related to the composition, structure, and growth mechanism of the coatings.

The largest hardness at 490 °C is due to the elastic modulus difference between the coatings at different temperature. According to the critical load ($L_c$) shown in Table 3, the critical load ($L_c$) observed from that 490 °C sample is larger than those on the 470 and 510 °C ones. The high hardness is related to the role of the interfaces as effective obstacles for lattice dislocation slip and the dominant deformation mechanism in nanostructured coating [9,10]. Moreover, the interfaces may depend on the thermo dynamical equilibrium conditions and deposition temperature. Hence, the hardness increases at 490 °C, because the thermo dynamical equilibrium conditions are fulfilled at this temperature leading to the formation of pure TiC (see Figs. 1 and 2). On the other hand, Fig. 3 exhibits that a higher deposition temperature changes the growth mechanism. As a result, a columnar structure observed at 470 °C transforms in to a layered structure at 490 °C and 510 °C. Increasing the deposition temperature enhances the hardness due to the larger interface density and the smaller grain size based on the Hall–Petch effect [27–29].

The Young's modulus versus temperature relationship is depicted in Fig. 6. The area function of this indenter is calibrated using B270 glass and the elastic modulus is determined independently using the pulse-echo method [17–19].

The Young's moduli of the TiC coatings deposited at 470, 490, and 510 °C are 289.9, 400 and 187.6 GPa, respectively. The 490 °C sample has the largest Young's moduli (E) and its mechanical

**Table 3**
Grain size and mechanical properties of the nanostructured $TiC_x$ coatings deposited at 470, 490, and 510 °C.

| Operating temperature (°C) | Grain size (nm) | Critical load (mN) | $H$ (GPa) | $E$ (GPa) | $\mu$ | $R_a$ (nm) | $R_{rms}$ (nm) |
|---|---|---|---|---|---|---|---|
| 470 | 15 | 28 | 16.47 | 289.9 | 0.268 | 10.203 | 13.069 |
| 490 | 7 | 34 | 16.62 | 400 | 0.23 | 24.376 | 29.781 |
| 510 | 5 | 21 | 12.78 | 187.6 | 0.39 | 8.992 | 11.668 |

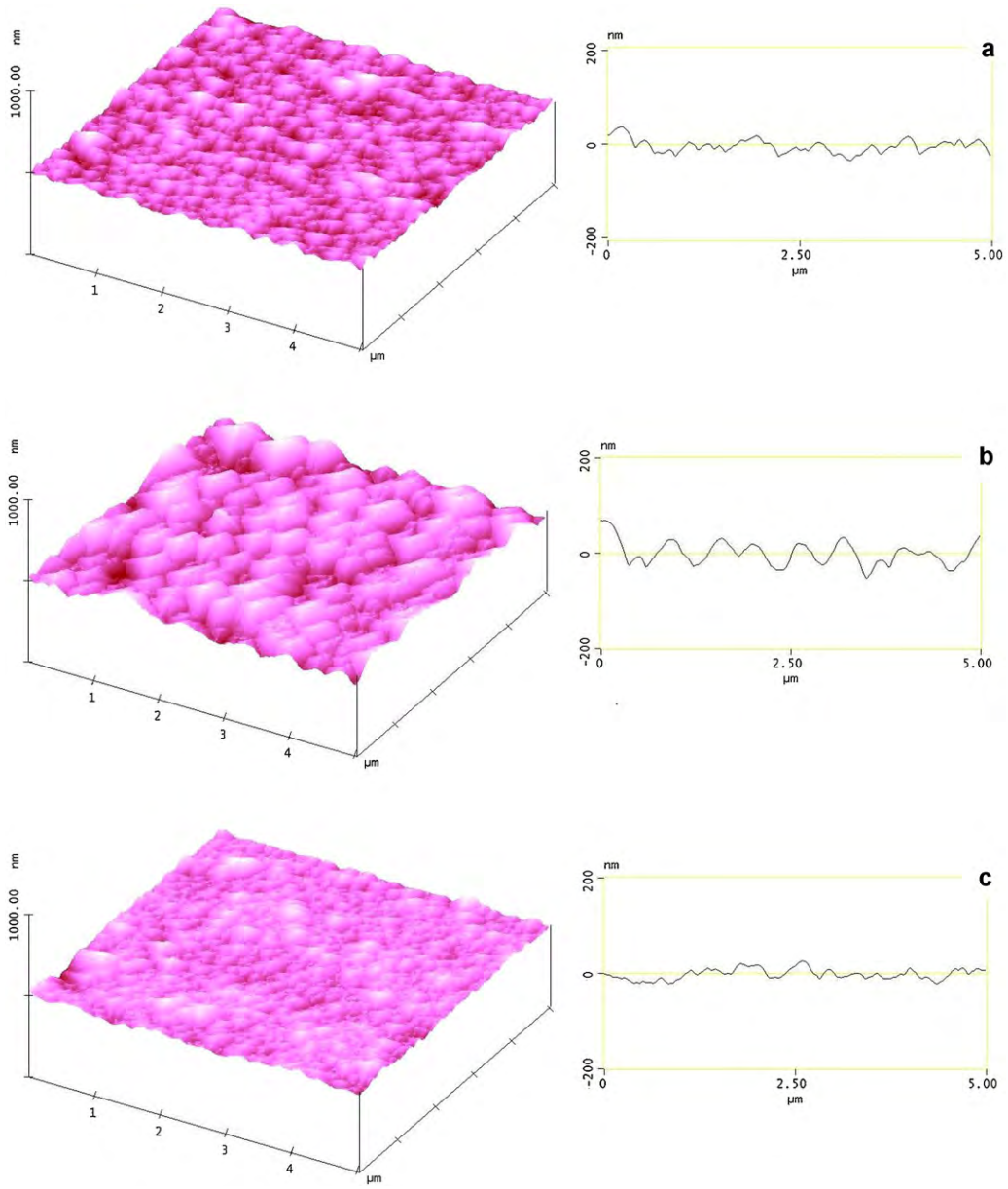


**Fig. 3.** Topographic data (images and surface profiles) of the TiC coatings deposited at different temperatures: (a) 470 °C, (b) 490 °C, (c) 510 °C.

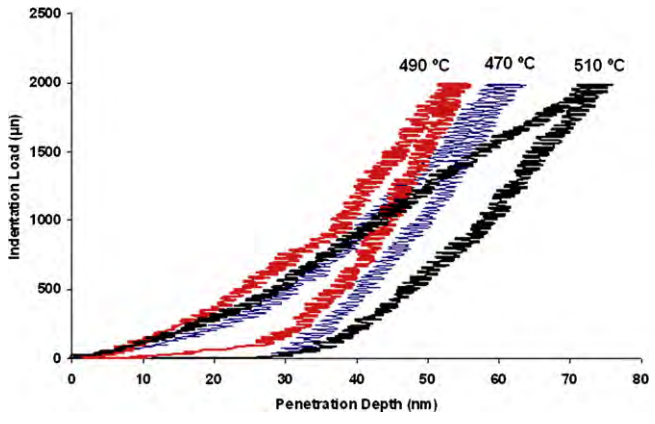


**Fig. 4.** Load–unloading curves of the TiC coatings deposited at 470, 490, and 510 °C.

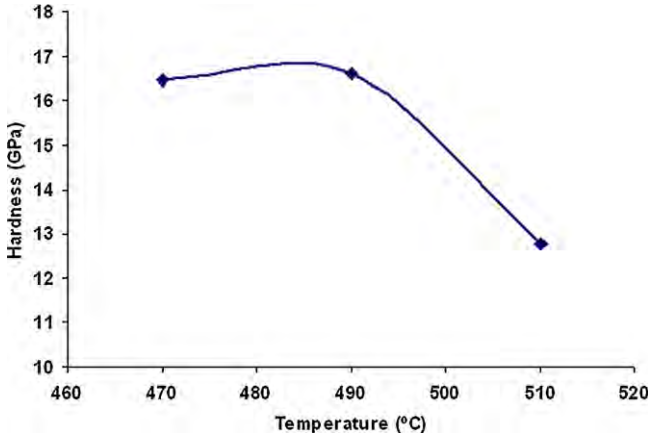


**Fig. 5.** Hardness of TiC coatings as a function of the deposition temperature.

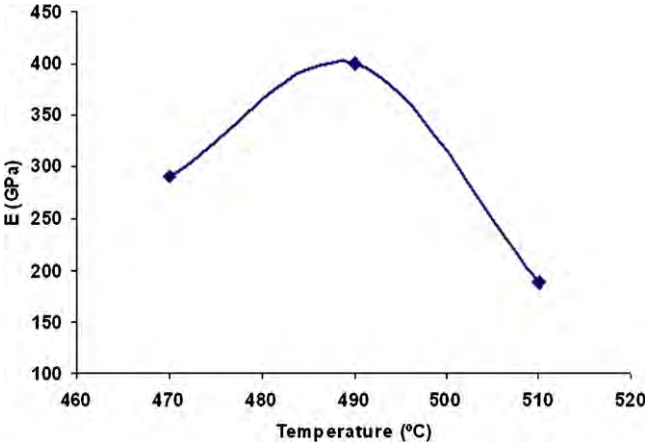


**Fig. 6.** Young's modulus of TiC coatings as a function of the deposition temperature.

response is expected to be more elastic and a higher component of elastic response may account for the slightly higher hardness value (400 GPa) compared the samples produced at 470 and 510 °C. This higher elastic modulus and hardness of the 490 °C sample can be attributed to the presence of nanocrystalline stochiometric titanium carbide (TiC) and the results are summarized in Table 3.

Fig. 7a–c shows the surface morphology of the residual scratches and the variation of the friction coefficients with time. Based on the nanoscratch data, changes in the relative elastic–plastic response can be monitored. The friction coefficient ($\mu$) defined as the average ratio of the lateral (friction) force to the normal force is shown in Table 3.

The coating deposited at 490 °C exhibits a lower friction coefficient, and the AFM surface morphologies of the residual scratches reveal plastic deformation at 470 and 510 °C but elastic response at 490 °C. The hardness (H) is essentially a measure of the resistance to plastic deformation and so harder materials have inherently higher resistance to plowing [30].

In order to determine the wear mechanism, the morphology of the worn surfaces is examined by AFM images as shown in Fig. 7.

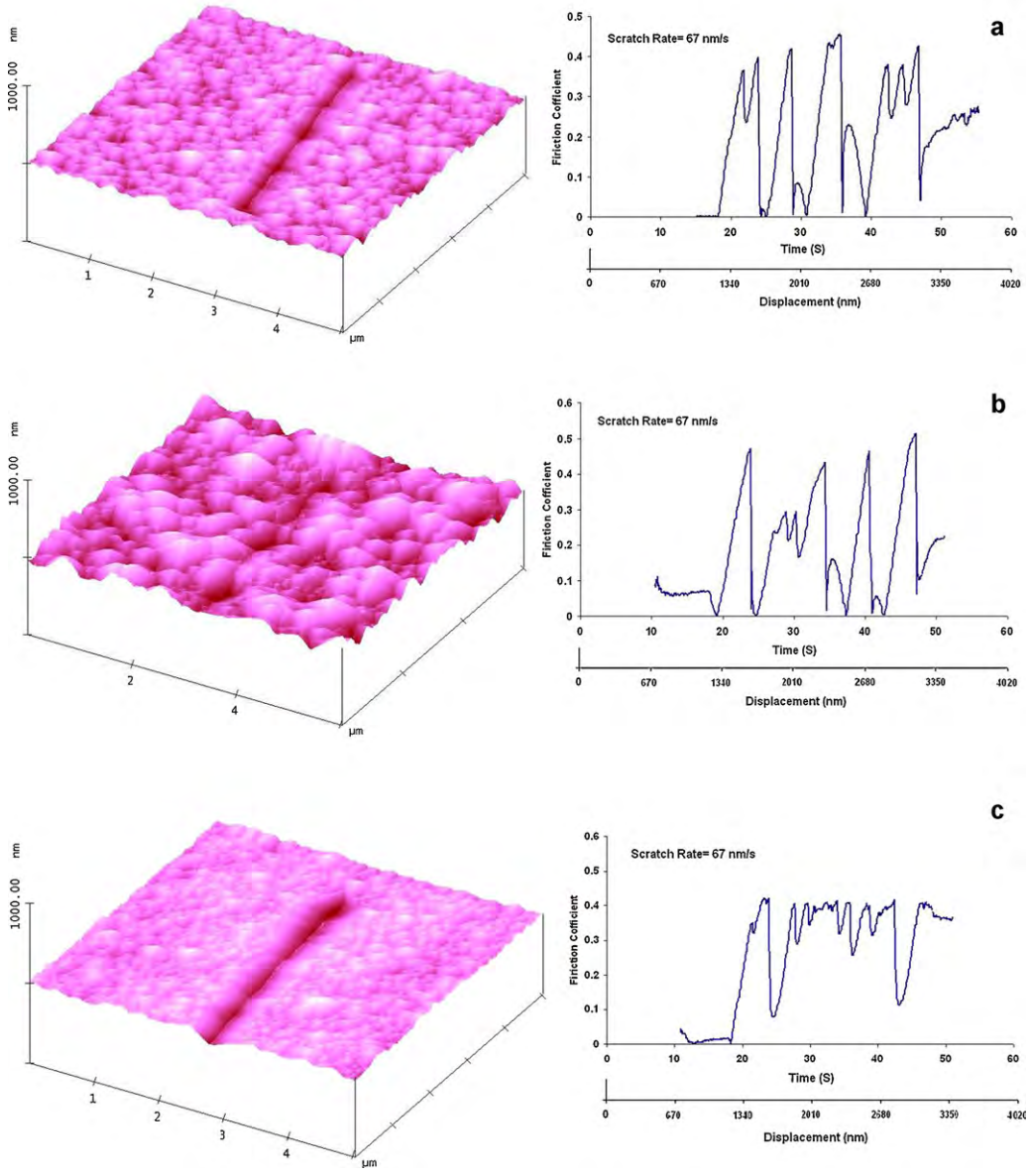


**Fig. 7.** AFM surface morphologies of the residual scratches and variations in the frictional coefficient versus time: (a) 470 °C, (b) 490 °C, and (c) 510 °C.

The wear track consists of mainly grooves, and the width of the wear track decreases with increasing hardness. A small amount of materials pushed up outside the grooves can be observed on the worn track of the 490 °C sample. Materials transfer occurs during sliding and the materials are transferred to the worn surfaces. When the deposition temperature increases from 490 °C to 510 °C, plowing can be clearly observed on the worn surface and this behavior is seen when the deposition temperature is reduced from 490 °C to 470 °C. This may be attributed to the growth mechanism and compressive residual stresses in the coating at the three deposition temperatures.

The increase in the friction coefficient ($\mu$) measured from the TiC coating deposited at 490 °C can be explained by the running-in behavior of the coating–tip interface. During the running-in, owing to the interaction between the tip and asperities on the coating, the friction coefficient ($\mu$) rises. It can be concluded that the growth mechanism plays an important role in the variation of the friction coefficients. The layer growth decreases the intrinsic friction coefficient and increases the apparent friction coefficient, compared to island growth under the same composition. The results indicate that the dominant nanoscratch mechanism involves plowing and materials transfer [31].

## 4. Conclusion

Nanostructured TiC are deposited on hot-working tool steel ($H_{11}$) by PACVD at 470, 490, and 510 °C and AFM is used to determine the composition, microstructure, and nanomechanical properties. Pure TiC (without $TiO_2$) coatings are deposited at 490 °C. The apparent grain sizes calculated from Scherrer equation are 13, 7, and 8 nm for the 470, 490 and 510 °C samples, respectively. The $R_{rms}$ values of the coatings deposited at 470, 490, and 510 °C are 13.069, 29.781 and 11.668 nm, respectively. A higher deposition temperature reduces the surface roughness. A different growth mechanism at 490 °C increases the $R_{rms}$ compared the samples fabricated at 470 and 510 °C. The dominant mechanism of growth structure at 490 °C is layer type, whereas that at 470 and 510 °C is island type. Optimization of the deposition parameters such as the operating temperature allows fine-tuning of the homogeneity, density, structure, and tribological properties of the coating. The hardness of the coatings reaches a maximum of 16.62 GPa at 490 °C and then decreases at 510 °C because the thermo dynamical equilibrium conditions are met at 490 °C thereby producing pure TiC. The Young's moduli of the 470, 490, and 510 °C samples are 289.9, 400, and 187.6 GPa, respectively. The larger elastic modulus and hardness of the 490 °C coating can be attributed to the presence of nanocrystalline TiC. The TiC coating fabricated at 490 °C exhibits lowest friction coefficient and AFM conducted on the residual scratches shows plastic deformation on the 470 and 510 °C coatings but elastic response on the 490 °C one. The proper operating temperature in the PACVD process not only yields a smooth and fine-grained morphology, but also improves the tribological behavior and mechanical properties, especially on the nano scale.

## Acknowledgements

The authors would like to express their thanks to Iranian Nanotechnology Initiative Council. The work was financially supported by Hong Kong Research Grants Council (RGC) General Research Funds (GRF) No. CityU 112510 and City University of Hong Kong Applied Research Grant Nos. 9667038 and 9667066.

## References

[1] L.R. Katipelli, A. Agarwal, N.B. Dahotre, Appl. Surf. Sci. 153 (2000) 65–78.
[2] S. Inoue, Y. Wada, K. Koterazawa, Vacuum 59 (2000) 741.
[3] A. Mani, P. Aubert, F. Mercier, H. Khodja, C. Berthier, P. Houdy, Surf. Coat. Technol. 194 (2005) 190–195.
[4] A.C. Fernandes, P. Carvalho, F. Vaz, S. Lanceros-Méndez, A.V. Machado, N.M.G. Parreira, J.F. Pierson, N. Martin, Thin Solid Films 515 (2006) 866–871.
[5] A. Leonhardt, K. Bartsch, I. Endler, Surf. Coat. Technol. 76–77 (1995) 225–230.
[6] I. Dahan, A. Admon, N. Frage, J. Sariel, M.P. Dariel, J.J. Moore, Surf. Coat. Technol. 137 (2001) 111.
[7] B.D. Cullity, Elements of X-ray Diffraction, second ed., Addison Wesley, 1978.
[8] A. Niederhofer, T. Bolom, P. Nesladek, K. Moto, Ch. Eggs, D.S. Patil, S. Veprek, Surf. Coat. Technol. 183 (2001) 146–147.
[9] M. Sakurai, T. Toihara, M. Wang, W. Kurosaka, S. Miyake, Surf. Coat. Technol. 203 (2008) 171–179.
[10] E. Meyer, E. Gnecco (Eds.), Fundamentals of Friction and Wear on the Nanoscale, Springer-Verlag, 2007.
[11] R. Colaco, Wear 267 (2009) 1772–1776.
[12] W. Gulbiński, T. Suszko, D. Pailharey, Wear 254 (2003) 988–993.
[13] T.-H. Te-Hua Fang, S.-R. Jian, D.-S. Chuu, Appl. Surf. Sci. 228 (2004) 365–372.
[14] M. Sakuraba, D. Muto, M. Mori, K. Sugawara, J. Murota, Thin Solid Films 517 (2008) 10–13.
[15] Y. Zhu, W. Wang, X. Jia, T. Akasaka, S. Liao, F. Watari, Appl. Surf. Sci. (2012).
[16] S.H. Lee, K.H. Nam, S.C. Hong, J.J. Lee, Surf. Coat. Technol. 201 (2007) 5211–5215.
[17] W.C. Oliver, G.M. Pharr, J. Mater. Res. 7 (1992) 1564–1583.
[18] M.L. Oyen, J. Biomech. 39 (2006) 2699–2702.
[19] I. Pollini, A. Mosser, J.C. Parlebas, Phys. Rep. 355 (2001) 1.
[20] TriboScope® Users Manual of Hysitron Inc., 1999.
[21] L. Hultman, J.E. Sundgren, J.E. Greene, D.B. Bergstrom, I.J. Petrov, Appl. Phys. 78 (1995) 5395.
[22] E. Vogelzang, J. Sjollema, H.J. Boer, J.T.M. De Hosson, J. Appl. Phys. 61 (1987) 4606.
[23] D. Galvan, Y.T. Pei, J.Th.M. De Hosson, Acta. Mater. 53 (2005) 3925–3934.
[24] A.A. El Mel, B. Angleraud, E. Gautron, A. Granier, P.Y. Tessier, Thin Solid Films 519 (2011) 3982–3985.
[25] A. Kumar, H.L. Chan, J.S. Kapat, Appl. Surf. Sci. 127–129 (1998) 549.
[26] Y. Leprince-Wang, K. Yu-Zhang, Surf. Coat. Technol. 140 (2001) 155–160.
[27] K.N. Andersen, E.J. Bienk, Surf. Coat. Technol. 219 (2000) 123.
[28] H.G. Prengel, P.C. Jindal, K.H. Wendt, A.T. Santhanam, P.L. Pedge, R.M. Penich, Surf. Coat. Technol. 25 (2001) 139.
[29] S.G. Harris, A.C. Vlasveld, E.D. Doyle, P.J. Dolder, Surf. Coat. Technol. 383 (2000) 133.
[30] A. Chatterjee, N. Kumar, J.R. Abelson, P. Bellon, A.A. Polycarpou, Wear 265 (2008) 921–929.
[31] J. An, Q.Y. Zhang, Mater. Char. 58 (2007) 439–446.